

Self-Organised Criticality in the Oslo Model

Nikolaos Koukoulekidis

CID: 00950301

February 20, 2017

Abstract: Self-organised criticality was investigated via study of the Oslo model. The height of the pile of the model and the crossover time were found to scale with system size L and L^2 respectively. The average height of the steady state probability and avalanche size probability were found to collapse across system sizes. The avalanche size increased indefinitely with system size, indicating criticality. The pile was also observed to self-organise its average steady state slope to a constant limiting value.

Word count: 2380 words in report (excluding front page, figure captions and bibliography)

1 Introduction

Many open natural systems like sand dunes and earthquakes [1] present self-organised criticality. This is a characteristic property of non-equilibrium systems and refers to their tendency to slowly reach a steady state without any change in their control parameters [2]. This report studies the Oslo model which can describe a rice pile driven by addition of rice grains [3] which form avalanches. The system eventually self-organises to a non-equilibrium steady state in which the number of grains added to the system equals to the number of grains leaving as seen in figure (1). As the system size L grows, there is no characteristic size of avalanches and the system is called ‘critical’ [4].

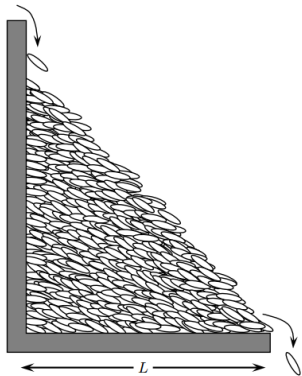


Figure 1: Sketch of the setup for the rice pile experiment [3]. Rice grains added drive avalanches and the system eventually reaches a non-equilibrium steady state in which grains entering the system are equal in number to grains leaving it. The finite system size L limits the avalanche size.

In order to study interesting features of similar systems in more detail, the Oslo model is introduced. It approximates the rice pile of figure (1) as a discrete one dimensional lattice consisting of L sites $i = 1, 2, \dots, L$. Each site is described by a number of grains h_i , a slope $z_i = h_i - h_{i+1}$ which indicates how many more grains the site has compared to the one on the right and a threshold slope $z_i^{th} \in \{1, 2\}$ which is assigned randomly with probability p for $z_i^{th} = 1$. The algorithm consists of three steps which are iterated. The lattice is initialised in the empty configuration and all threshold slopes are assigned. Then it is driven by adding a grain at the first site. In the last step, all sites with slope above the threshold, $z_i > z_i^{th}$ relax by moving a grain to the next site, or dropping it out of the system if the site is the last one. Slopes are adjusted accordingly and a new threshold slope is assigned to a site immediately after it relaxes. This repeats until all sites are relaxed. The number of relaxations defines the size of the avalanche s caused by the added grain. The height of the first site defines the height of the lattice h in the new configuration achieved due to the relaxation. Finally the number of sites L defines the system size.

Several aspects of the Oslo model are investigated in this report in an attempt to capture universal patterns for self-organised critical systems like the rice pile experiment. The height of the lattice and the avalanche size are the two observables that dominate the analysis. All the trends with system size and scaling relations observed are reported with the aim to explain a possible theoretical framework consistent with observations.

2 Results and Discussion

The model allows for flexibility in the threshold slope probability. Figure (2) illustrates a system of size 64 that has reached a steady state with different probabilities. The two

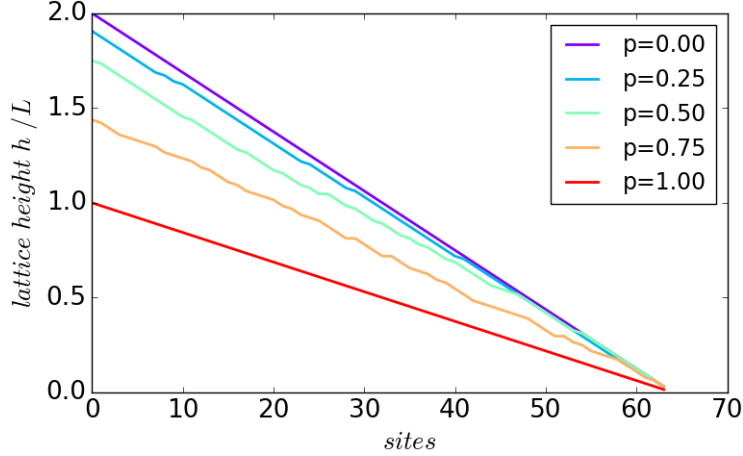


Figure 2: The Oslo model for system size $L = 64$. Adjusting the threshold probability has a clear effect on the slope of the recurrent configurations of the system. BTW models for $p = 0$ or 1 exhibit no fluctuations in the slope unlike the model for a probability in between. Average slopes are calculated $\bar{z} = 1, 1.44, 1.75, 1.91, 2$ respectively for increasing probability.

extreme cases of $p = 0$ and 1 only have one possible steady state which corresponds to a slope of 2 or 1 throughout the sites respectively, as described by the simpler BTW model [5] and thus the system takes a perfect triangular shape. A probability between 0 and 1 allows for two different slope values at each site and therefore induces some fluctuations in the shape of the system and its height h , leading to the concept of average lattice height \bar{h} . The average slope of the system $\bar{z} \equiv \frac{\bar{h}}{L}$ is expected to be bounded between the extremes 1 and 2 . Interestingly, $p = 0.5$ leads to an average slope which is higher than 1.5 , in fact $\bar{z} \approx 1.75$ in this simulation. This can be explained by the fact that sites with $z_i^{th} = 1$ tend to relax more often, since they can hold one fewer grain, thus the system has the tendency to consist of more sites with threshold slope of 2 . In the steady state, the influx of grains needs to equal the outflux, thus all possible grain positions are occupied and that the threshold slopes translate into actual slopes. In fact, an average slope of 1.5 is only achieved near $p = 0.70$ for $z_i^{th} = 1$, as suggested by figure (2).

2.1 Lattice Height

The system starts from the empty state and, as grains are added, it moves through transient configurations until it reaches the recurrent configurations which constitute the steady state of the system. The number of grains needed to reach the steady state is called the crossover time t_c . Figure (3) shows how the system ‘self-organises’ into the steady state for different system sizes. Since the threshold slope values are not fixed, there are multiple recurrent configurations and the system can be seen in the figure to fluctuate among them, remaining close to an average lattice height.

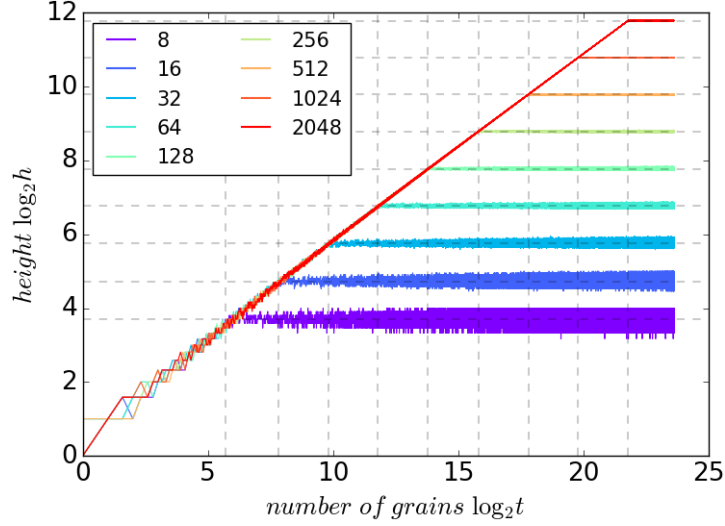


Figure 3: Plot of $\log_2 h - \log_2 t$, where t is the number of grains added in the system. Cross over times t_c and average steady state heights \bar{h} differ by 2 and 1 respectively between systems of different sizes. The fluctuations between recurrent configurations are more evident for small system sizes, because of the nature of a loglog plot.

The system sizes are powers of 2, hence plotting a loglog plot in base 2 reveals some information about scaling with system size. Firstly, the behaviour of height during the transient states seems to follow the same power law regardless of system size with exponent approximately 0.5 as can be found by estimating the slope of the overlapping plots up to t_c . The dashed lines can be used to estimate how \bar{h} and t_c grow as L doubles. The lines are equidistant in the loglog plot with a distance of 1 and 2 for average steady state height and crossover time respectively. This suggests

$$\begin{aligned}\bar{h}(2L) &= 2\bar{h}(L) \Rightarrow \bar{h} \propto L \\ t_c(2L) &= 4t_c(L) \Rightarrow t_c \propto L^2\end{aligned}$$

These relations can be understood by considering the geometry of the system after enough iterations. As seen in figure (2), the steady state of a system tends to have a constant average slope $\bar{z} \approx 1.75$ and the triangular shape of the pile in the figure with perpendicular sides \bar{h} and L suggests that $\bar{h} = \bar{z}L$, being consistent with the definition of average slope. This triangle has an area $\frac{1}{2}\bar{z}L^2$, thus bounded between $\frac{1}{2}L^2$ and L^2 . This represents the number of grains, which is conserved in the steady state. The explanation agrees with the corresponding numerical results of figure (4).

This analysis suggests that the average height and crossover time are characteristic scales for each system size and that the data can collapse, so that

$$h = \bar{h}\mathcal{F}\left(\frac{t}{t_c}\right) \quad \text{or} \quad \frac{h}{L} = \mathcal{F}\left(\frac{t}{L^2}\right) \quad (1)$$

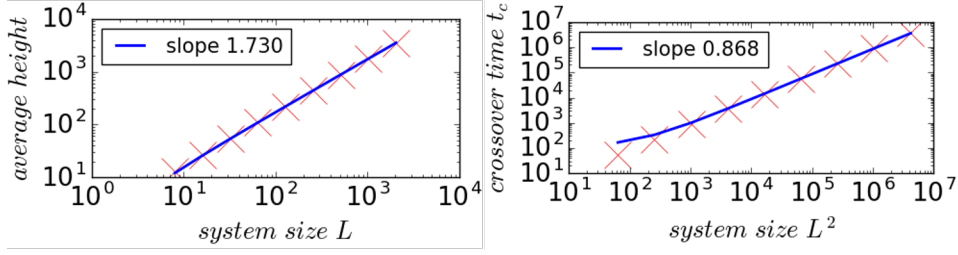


Figure 4: Scaling of average steady state height \bar{h} and cross over time t_c with system size L . The slope of the crossover time plot is half the slope of the height plot which is approximately the average slope estimated in figure (2).

which is plotted in figure (5). The data, which have been smoothed out by a central moving average, indeed collapse and the plot reveals some properties of the scaling function $\mathcal{F}(x)$. The crossover points overlap for all systems at a point in the plot, defining the two different behaviours of the scaling function.

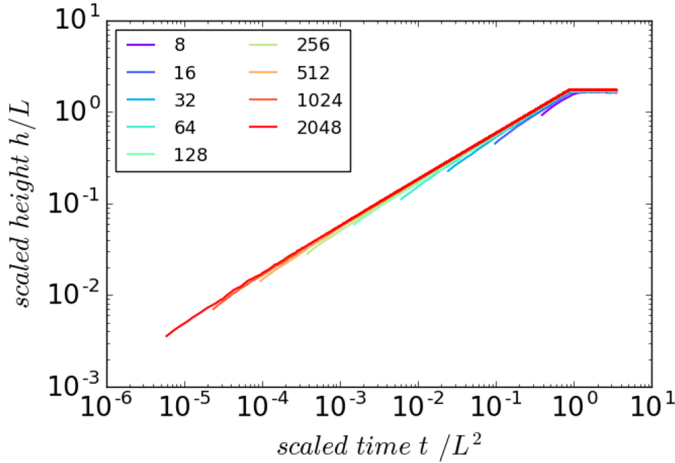


Figure 5: The scaling function between height and time (i.e. number of grains added). It grows as a square root in the beginning, but remains constant after the crossover time. The slope of the relation is 0.50(2) in agreement with the estimate in figure (3).

shows corrections to scaling, since in small systems random fluctuations in the average slope which determines the height are significant. Hence, a more accurate scaling formula for average height would be

$$\bar{h} = \alpha L(1 - \beta L^{-\omega_1} + \dots). \quad (2)$$

The slope of the left part of \mathcal{F} is 0.50 meaning that $h \propto t^{0.50}$ during the transient which seems reasonable considering that the number of grains is proportional to the area of the triangular pile. After the crossover time, the scaling relation is a constant, which follows from the height being approximately constant in the steady state. The system cannot grow any further because grains are conserved and the height cannot change much. Therefore,

$$\mathcal{F}(x) = \begin{cases} x^{0.5} & \text{if } t < t_c \\ \alpha & \text{if } t > t_c \end{cases}$$

The constant α characterises the behaviour of height for large L and is estimated in figure (4) close to 1.73. Although not obvious in the figure, the average height

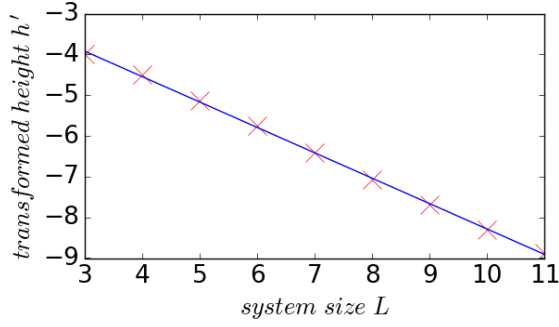


Figure 6: Corrections to scaling are well approximated to first order. The optimal parameters of the fitting are $(\alpha, \omega_1) = (1.73, 0.62)$.

Ignoring further corrections to scaling, the equation can be transformed into

$$h' \equiv 1 - \frac{\bar{h}}{\alpha L} = \beta L^{-\omega_1}.$$

which is plotted in figure (6). Parameter α is fine-tuned until the best linear fit is obtained which gives a slope $\omega_1 = 0.62$ in the loglog plot. This is not far from 1 and clearly the first order correction can be important for small sizes.

As system size increases, the number of recurrent configurations increases as well, therefore the number of possible \bar{h} rises. It is thus expected that the standard deviation of the average height σ_h increase with system size as confirmed in figure (7).

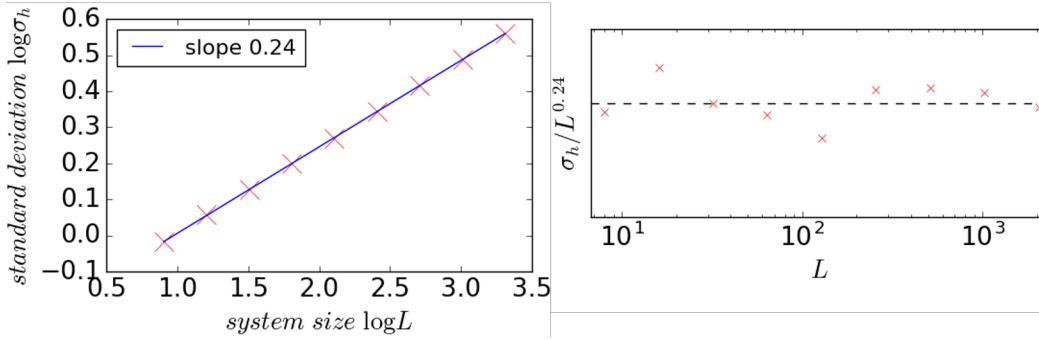


Figure 7: Standard deviation increases proportional to $\propto L^{0.24}$. It does not present corrections to scaling.

The standard deviation scales slowly with $L^{0.24}$ and seems to have no apparent corrections to scaling according to figure (7 right) which indicates no trend unlike for the average height in equation (2). Since $\bar{h} = \bar{z}L$, the standard deviation of the average slope is $\sigma_z = \frac{\sigma_h}{L}$. According to equation (2) and $\sigma_h \propto L^{0.24}$, as the system tends to become infinite in size,

$$\begin{aligned} \bar{z} &= \frac{\bar{h}}{L} \rightarrow \alpha = 1.73 \\ \sigma_z &= \frac{L^{0.24}}{L} \rightarrow 0 \end{aligned}$$

This shows that the system “self-organises” the slope of the pile to a specific value and is also consistent with the initial argument that this value is closer to 2 than 1, although the threshold slopes are assigned with 0.5 probability each.

Since the number of different heights in the steady state increases with system size, the probability distribution $P(h; L)$ of them cannot be identical from size to size. However, given that the system has iterated enough times, the central limit theorem forces the distribution to be Gaussian which will be rescaled according to the average height and standard deviation that correspond to the size. Defining the rescaled probability $\tilde{P} \equiv \sigma_h P$ and the rescaled height $z \equiv \frac{h - \bar{h}}{\sigma_h}$, then all Gaussians can collapse to the standard normal distribution which has average 0 and standard deviation 1

$$P(h; L) = \frac{1}{\sqrt{2\pi}\sigma_h} e^{-\frac{h-\bar{h}}{\sigma_h}} \Rightarrow \tilde{P}(z; L) = \frac{1}{\sqrt{2\pi}} e^{-z^2/2}$$

The uncollapsed and collapsed distributions are illustrated in figure (8).

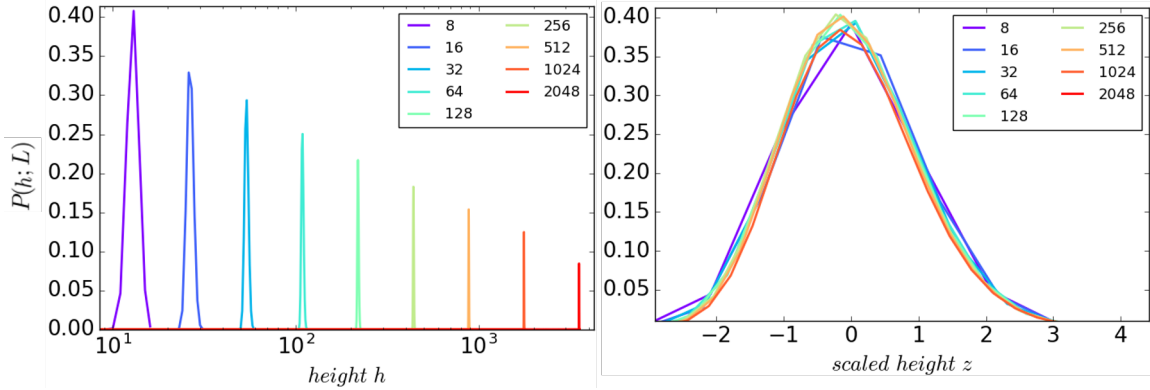


Figure 8: The probability distributions $P(h; L)$ of steady state height at a given system size are Gaussian which can collapse to the standard normal distribution.

2.2 Avalanche size

The most important feature of the avalanches is that as long as the system size is sufficiently large, the avalanche size remains unrestricted. While the system is finite, there is only a finite number of grains that can drop off, and the avalanche size is bounded. The avalanche size probability for a given system size $P(s; L)$ is an indicative measure of this system property. Figure (9) shows the probability distribution for various numbers of iterations on a system of size 2048. The more the iterations, the higher the number of large avalanches included in the data. The raw data are represented by the blue crosses in the figure. Data log-binning [4] is applied yielding the green lines, to extract more information from the noisy tails of the probability distributions, where there are only very small sample sizes. Therefore, the cut-off avalanche size is artificially increased towards its correct value at the limit of infinite iterations. As a counterexample, 10^4 iterations in the top left graph, do not yield the low probabilities of large avalanches and cannot illustrate the cut-off. The bottom left figure with 10^6 iterations indicates a clear probability distribution. Lowering the base of the log-binning a results in more noisy data, which do not form a solid distribution, while increasing it much more than 1.2 results in bins

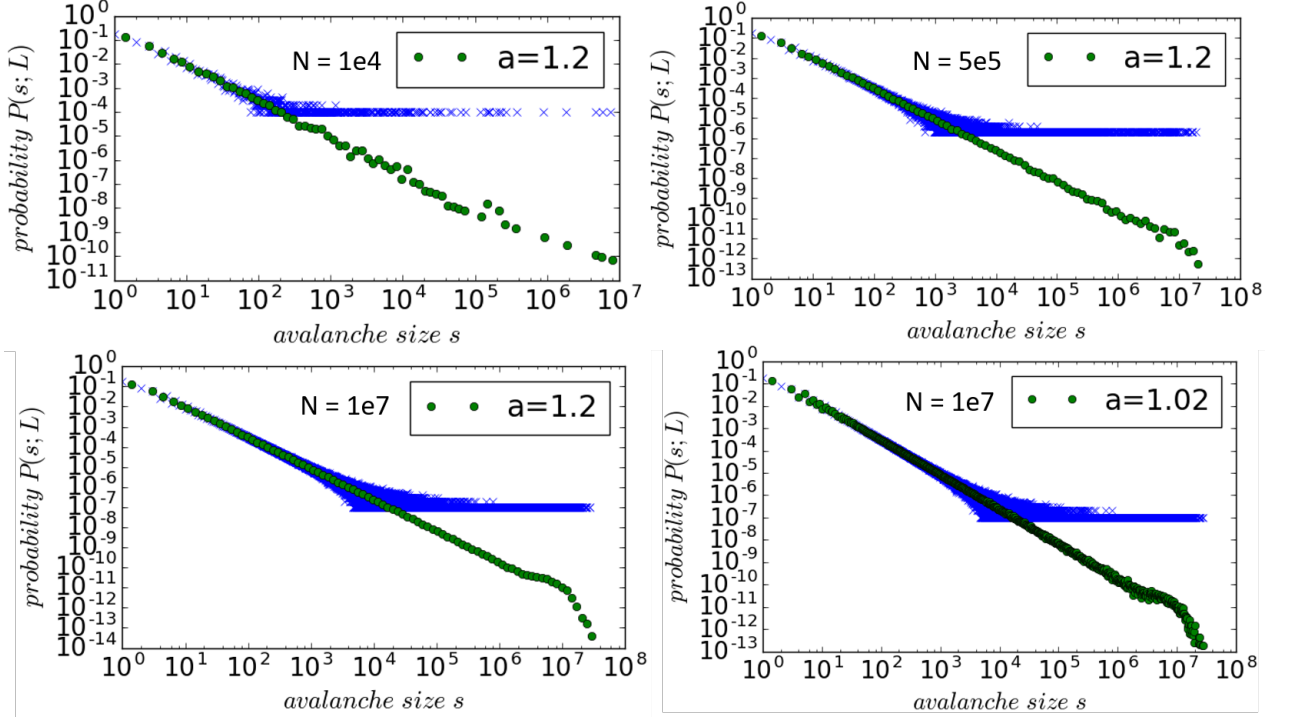


Figure 9: Top left: Log-binning of $N = 10^4$ avalanches with bin base $a = 1.2$. Top right: $(N, a) = (5 \times 10^5, 1.2)$. Bottom left: $(N, a) = (1 \times 10^7, 1.2)$. Bottom right: $(N, a) = (1 \times 10^7, 1.04)$. The avalanche size cutoff increases with the number of iteration as more large avalanches are captured in the data. Optimal bin base was found to be close to 1.2.

containing too many data points producing very sparse bins and thus losing information.

Using $N = 10^7$ the log-binned avalanche size probability is plotted against size for all system sizes in figure (10 left). Larger systems have a cut-off at higher avalanche sizes as expected, but the cut-offs are equidistant as is the case with time and height in figure (3). This distance in a loglog graph of base 2 is the “gap exponent” D which describes the dependence of the avalanche cut-off on system size. The probability distributions also have the same slope which corresponds to an exponent τ_s if measured as well, dictating the dependence of the probability on avalanche size. All this suggests a possible data collapse of the form

$$P(s; L) \propto s^{-\tau_s} \mathcal{G}\left(\frac{s}{L^D}\right) \quad (3)$$

The avalanche size cut-off increases indefinitely with system size indicating that there is no limit to the avalanche size for an infinite system. This characterises the criticality of the system.

Optimal estimation of the two exponents may be made by moment analysis, where

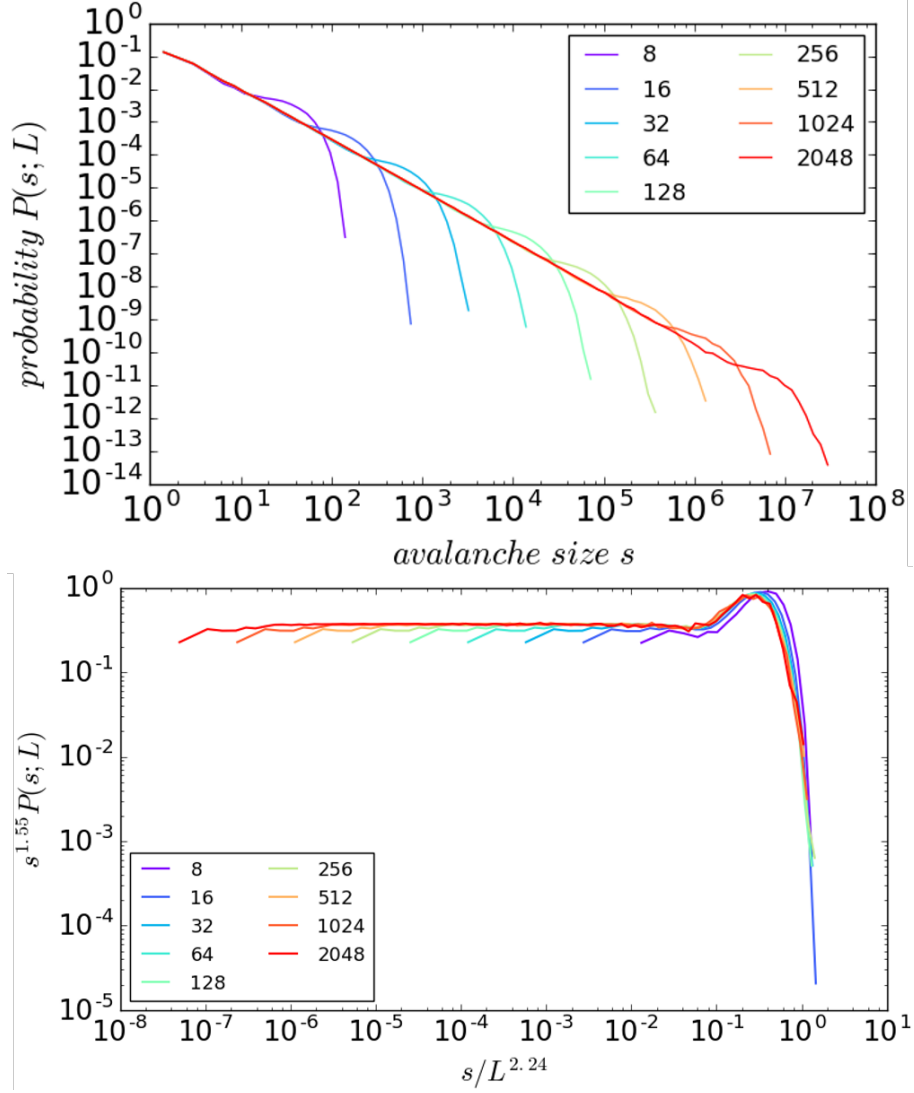


Figure 10: Avalanche size probability against size before and after collapse with exponents $(D, \tau_s) = (2.24, 1.55)$. The pile tends to become critical as system size increases since the avalanche cut-off increases indefinitely.

the k^{th} moment of the system is defined as

$$\bar{s}^k = \sum_{s=1}^{\infty} s^k,$$

and s is the avalanche size.

Using the finite size scaling ansatz described by equation (3) the system size dependence of the k^{th} moment can be estimated.

$$\begin{aligned}
\bar{s}^k &= \sum_{s=1}^{\infty} s^k P(s; L) \\
&= \sum_{s=1}^{\infty} s^{k-\tau_s} \mathcal{G}\left(\frac{s}{L^D}\right) && \text{ansatz} \\
&\propto \int_1^{\infty} s^{k-\tau_s} \mathcal{G}\left(\frac{s}{L^D}\right) ds && s \gg 1 \\
&= \int_{\frac{1}{L^D}}^{\infty} (L^D u)^{k-\tau_s} \mathcal{G}(u) du && u = \frac{s}{L^D} \\
&= L^{D(1+k-\tau_s)} \int_{\frac{1}{L^D}}^{\infty} (u)^{k-\tau_s} \mathcal{G}(u) du \\
&= L^{D(1+k-\tau_s)} \int_0^{\infty} (u)^{k-\tau_s} \mathcal{G}(u) du && L \gg 1
\end{aligned}$$

Therefore, $\bar{s}^k \propto L^{D(1+k-\tau_s)}$. This is very useful, since the moments are easily calculated by the avalanche size measurements. In the particular case of $k = 1$, grain conservation in the steady state yields a scaling relation. Potential energy added to the system by new grains is proportional to the average height and thus system size, while energy leaving the system is proportional to the avalanche size since the avalanches drive the grains. Therefore, $\bar{s} \propto L \Rightarrow D(2 - \tau_s) = 1$. The estimates of the exponents fulfill this relation.

In general, the slope of the graph $\log \bar{s}^k$ against $\log L$ gives an estimate for $D(1+k-\tau_s)$ which in turn can be plotted against the moment order k as done in figure (11 left) to allow for calculation of the exponents, since the slope is D and the y-intercept is $D(1-\tau_s)$. Care needs to be taken in deciding which moments to use for analysis. Moments of high order k are impractical leading to extremely large numbers for large avalanche sizes leading to outliers. Figure (11 right) tests the fifth order moment which is the most volatile to show that moments are also affected by corrections to scaling. Hence, excluding low system sizes from the calculations improves exponent estimates.

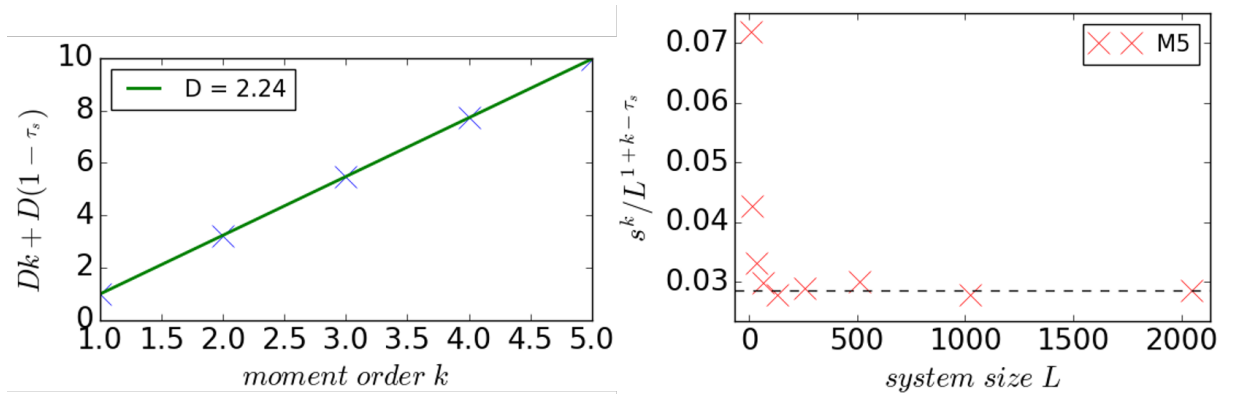


Figure 11: Moment analysis gives $(D, \tau_s) = (2.242, 1.556)$. Moments illustrate signatures of corrections to scaling.

2.3 Drop probability

The same analysis can be performed to investigate the probability of d grains leaving the system $P(d; L)$. Figure (12) shows the distribution before and after the collapse. The drop

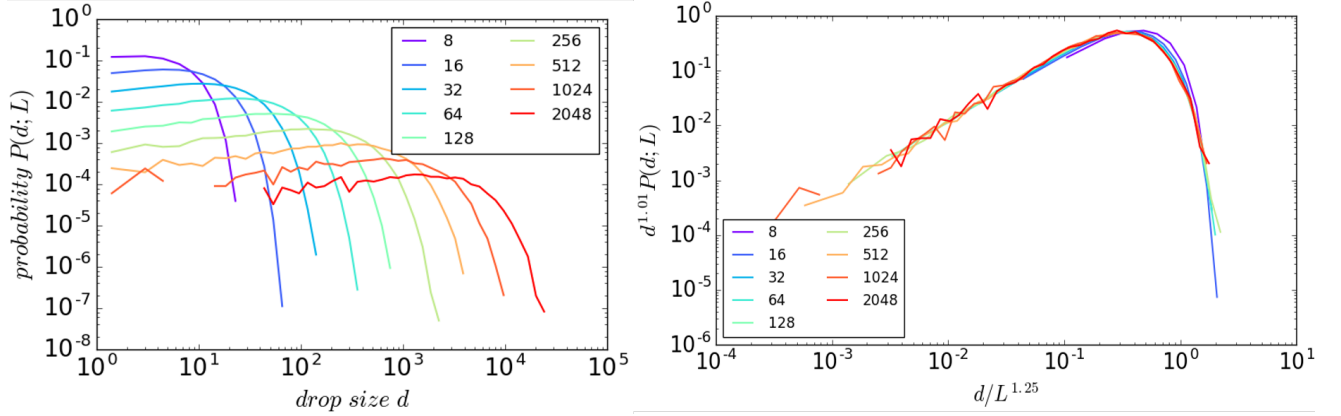


Figure 12: Moment analysis gives $(D, \tau_d) = (1.25, 1.01)$. The drops collapse to a very different function from the avalanches. Moments of drop sizes also illustrate signatures of corrections to scaling.

size probability has a rapid cut-off which occurs at larger number of grain drops as system size increases. This is again evidence of criticality for the system and indicates that an infinite system can have a large amount of grains leaving the system at a correspondingly low probability to normalise the distribution. Moment analysis leads to the probability collapsing in the scaling relation

$$P(d; L) \propto d^{-1.01} \mathcal{H}\left(\frac{d}{L^{1.25}}\right),$$

where $\mathcal{H}(x)$ has the functional form depicted in figure (12 right).

3 Conclusion

The aim of the project was to implement the Oslo model and simulate systems that present evidence of self-organised criticality. The behaviour of the height of the system lattice, the avalanche-size probability and the grain drop probability were examined and found to be properties that indeed highlight self-organisation and criticality. Establishing scaling forms for the height and probabilities was the main evidence of these features.

Various other parameters of the model can also be tested like the average velocity of grain through the lattice [2] which can lead to a deeper understanding of the model. The universality of the exponents also needs to be tested in the search of a broader theory for self-organised criticality.

References

- [1] K. Christensen, *Slides for Networks course*, Physics Dept., Imperial College London, 2014, downloaded from Blackboard 2nd February 2015.
- [2] K. Christensen *et al.*, “Avalanche Behavior in an Absorbing State Oslo Model”, Phys.Rev.E. **70** (2004) 067101.
- [3] K. Christensen *et al.*, “Tracer dispersion in a self-organized critical system”, Phys.Rev.Lett. **77** (1996) 107-110.
- [4] K. Christensen and N.Maloney, *Complexity and Criticality*, Imperial College Press, London, 2005.
- [5] P. Bak et al., *Self-Organized Criticality: An Explanation of 1/f Noise*, Phys. Rev. Lett. (1987) 59:381.